EEG Modulations Induced by a Visual and Vibrotactile Stimulation

Gabriela Herrera Altamira, Stéphanie Fleck, Anatole Lécuyer, Laurent Bougrain

EEG Modulations Induced by a Visual and Vibrotactile Stimulation

1st Gabriela Herrera Altamira
Neurorhythms team
Université de Lorraine, CNRS, LORIA, F-54000
Nancy, France
gabriela.herrera-altamira@loria.fr

2nd Stéphanie Fleck
PErSEUs
Université de Lorraine F-57073
Metz, France
stephanie.fleck@univ-lorraine.fr

3rd Anatole Lécuyer
Hybrid Team
University of Rennes, Irisa, UMR CNRS 6074
Rennes, France
anatole.lecuyer@inria.fr

4th Laurent Bougrain
Neurorhythms team
Université de Lorraine, CNRS, LORIA, F-54000
Nancy, France
laurent.bougrain@loria.fr

***Abstract*—Kinesthetic motor imagery (KMI) based brain-computer interfaces hold great potential for post-stroke motor rehabilitation. However, KMI is a complex task to perform, mainly due to the absence of sensory and kinesthetic feedback. To address this issue, sensory neurofeedback solutions have been proposed. One of them is tactile vibration, which has been used in BCI paradigms, but the optimal design choices of the vibration remain unclear. In this study, we present a novel bimodal stimulus that combines a vibrotactile device for the upper limb with a visual animation of a hand grasping a bottle. We aimed to investigate the effects of four different vibration patterns and four stimulation intensities to study the effects of the stimuli on the electroencephalography (EEG) signals of 17 healthy subjects without performing KMI. Our findings revealed EEG activity in the alpha, beta, and delta frequency bands within the somatosensory cortex during the sensory stimulation. While we did not observe significant differences in brain activity among the vibration patterns, we did observe statistically significant variations based on the vibration intensity. We observed central activity in both brain hemispheres, with stronger activity occurring in the contralateral hemisphere. Additionally, EEG activity seemed to involve the contralateral occipital areas. Based on these results, it is worth considering the delivery of feedback after participants have completed KMI tasks to differentiate and comprehensively study the brain activity resulting from the mental and sensory stimulation tasks.**

***Index Terms*—visual stimulation, vibrotactile stimulation, electroencephalography, brain-computer interface**

I. Introduction

Brain-computer interfaces (BCIs) are a promising technology for upper-limb motor rehabilitation of post-stroke patients. Electroencephalography (EEG)-based BCIs are commonly used due to their high spatial resolution, portability, and low cost [1]. Kinesthetic motor imagery (KMI), which involves imagining the sensations of a movement (e.g., pressure, temperature, roughness, muscular contraction), is a suitable BCI-control method for stroke patients who cannot physically move but can imagine it. Unlike visual motor imagery, KMI modulates sensorimotor cortical activity that can improve motor performance and aid in primary motor cortex rehabilitation [2]. However, KMI lacks sensory and kinesthetic feedback, which makes it challenging to execute and learn, posing challenges for system control. Various sensory feedback modalities, including functional electrical stimulation, tendon vibration, and tactile stimulation like tactile vibration, have been proposed to address this issue [1], [3].

Previous studies have shown that vibrotactile stimulation enhances motor imagery performance [4]. However, including vibration during motor imagery tasks makes it difficult to distinguish the EEG oscillations associated with motor imagery from those related to sensory stimulation. Both tendon vibration [5] and tactile vibration [6] elicit EEG activity in the mu and beta bands. Therefore, differentiating between EEG modulations arising from sensory stimulation and those linked explicitly to KMI is crucial for motor rehabilitation BCIs. These EEG modulations manifest as event-related desynchronizations (ERD) or synchronizations (ERS), which illustrate the alterations in the activity of local interactions between main neurons and interneurons that govern the frequency components of the ongoing EEG. The former involves a decrease of power in a given frequency band while the latter indicates an increase of power, both probably due to a decrease/increase in synchrony of the underlying neuronal populations [7].

Furthermore, the specific characteristics of vibration used in studies remain unclear. Most vibrotactile feedback methods employ constant vibration intensity, but fMRI research has demonstrated intensity-dependent variations in the somatosensory cortex [8], suggesting potential differences in EEG responses. The order of activating and deactivating vibration motors is another important factor. For instance, one study simultaneously activated five vibration motors on the palm of

We acknowledge the support of the French National Research Agency (ANR), under grant ANR-19-CE33-0007 (project GRASP-IT).

each hand as feedback for right/left-hand MI [9], while another study sequentially activated six vibration motors placed on the neck [10]. The impact on EEG activity due to different activation patterns remains unclear.

Considering these factors, we conducted a study involving a novel bimodal stimulation combining a vibrotactile device for the upper limb with a visual animation depicting a hand grasping a bottle. Our objective was to investigate EEG modulations associated with four vibrotactile device configurations and four bimodal stimulation intensities. By focusing on sensory stimulation design, we aim to gain insights into the brain activity evoked by visual and vibrotactile stimuli, laying the groundwork for their potential use as feedback in KMI-based BCIs for post-stroke motor rehabilitation.

II. Material and Methods

A. Participants

We recruited 18 healthy right-handed subjects (9 female, mean age: 25.94 y/o, s.d.: 3.7) that participated voluntarily. They reported no medical history that could affect the task (i.e., diabetes, antidepressant treatment, or neurological disorders). All participants provided informed consent approved by the local ethical committee of Inria (COERLE, approval number: 2022-17)

B. Experimental setup

1) Vibrotactile Device: The non-invasive vibrotactile device consists of three 10 mm disc Eccentric Rotating Mass vibration motors (model B1034.FL45-00-015, Zhejiang Yuesui Electron Stock CO., LTD.) contained in 3D-printed cases and fixed on the forearm and the hand with adjustable bracelets. The motors are controlled by an Arduino Nano board using Pulse Width Modulation (PWM). The motors were named according to their positions: flexor (forearm), extensor (forearm), and hand (Fig.1(b)).

The final device is intended for the impaired upper limb of stroke subjects. Thus, performing the tests on the non-dominant limb may simulate this situation since recalling motor control and sensations is more complicated. The vibrotactile device was fixed on the non-dominant forearm and hand of the participants. They also held a bottle with their non-dominant hand, and the virtual hand that was presented was also the non-dominant. As all participants were right-handed, all tests involved the left upper limb. The participant's arm was placed on a pillow so the vibration would not propagate on a hard surface generating undesired stimuli.

2) Electroencephalographic recording: EEG signals were recorded with the OpenViBE software platform and a Biosemi Active Two 64-channel EEG system with a sampling rate of 2048 Hz. In accordance with the international 10-5 system, the EEG was recorded from 64 electrodes.

A screen was placed in front of the participants to present the virtual environment with instructions and the virtual hand movement (Fig.1(a)).

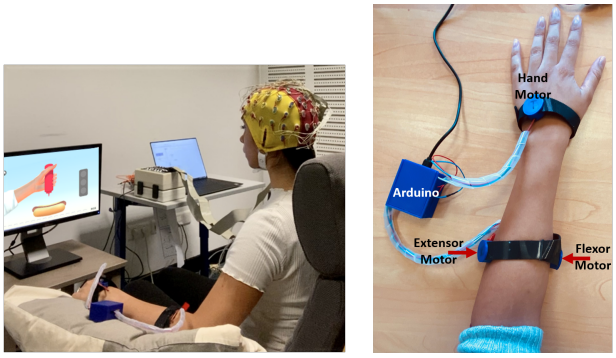

(a) Experimental Setup (b) Vibration motors

Fig. 1. Experimental setup overview with visual and vibrotactile stimulation using 3 (flexor, extensor, hand) or 2 motors (flexor, hand).

C. Experimental procedure

Each subject participated in a 90-minute session, consisting of a 30-minute preparation phase followed by one hour of bimodal stimulation, The stimulation phase was divided into four runs, where participants evaluated four different device configurations in a pseudo-randomized order. The evaluations were conducted using questionnaires and will be detailed in future publications due to lack of space.

Participants evaluated four different device configurations, varying in the number of vibration motors and vibration patterns. We proposed two configurations based on the number of motors: a) 3 motors (flexor, extensor, hand), and b) 2 motors (flexor and hand). Half of the participants started with three motors, while the other half started with two motors to avoid bias. In addition to the number of motors, participants evaluated two distinct vibration patterns. The first pattern, which we refer to as *Simultaneous pattern*, consists of the simultaneous activation and deactivation of all the motors, i.e. all motors are turned on/off at the same time. The second pattern called the *Sequential pattern* is inspired by the natural activation timing of the grasp muscles as described in [11]. Thus, the vibration started on the forearm and continued with the hand. The sequential activation pattern for three motors was: Flexor ON $\rightarrow$ Extensor ON $\rightarrow$ Hand ON $\rightarrow$ Hand OFF $\rightarrow$ Extensor OFF $\rightarrow$ Flexor OFF. For the two-motor configuration, the extensor motor was removed. The activation/deactivation time delay between motors was 400 ms. The order of presentation for the vibration patterns varied among participants.

The visual animation depicted a hand pressing a bottle of ketchup. First, the hand pressed the bottle, ketchup flows out from the bottle, and once the stimulation is over the hand opens to stop pressing the bottle. Four levels of ketchup quantity usually depend on the performance of the BCI, but for this study, the ketchup quantity is pseudo-randomized to match the expected number of trials. The vibration intensity and duration were proportional to the visual stimulus as described in Table I. Note the duration of the stimulation varies depending on the level. This discrepancy arises from

TABLE I
BIMODAL STIMULUS INTENSITIES AND DURATION

Trials	**Vibration Intensity**	**Visual animation**: ketchup quantity + hand movement	**Duration [seconds]**
4	None	None	2
4	Low PWM: 75; approx. 63.75 Hz	Small	2
4	Medium PWM: 150; approx. 127.45 Hz	Medium	4
4	High PWM: 225; approx. 191.18 Hz)	Large	6

the inherent need for a longer display time when a larger quantity of sauce is involved. Consequently, the inclusion of a lengthier visual animation contributes to enhancing the realism of the animation. The number of trials was balanced across all intensities and durations for improved offline statistics.

On the screen, a traffic light indicated the rest, preparation, and stimulation phases. The timeline of one trial was as follows: the traffic light was red for 30 seconds for participant rest and preparation to start the experiment. Then, it turned red and orange for 2 seconds, warning the participant the stimulation was about to start (preparation phase). Next, the traffic light remained orange during the bimodal (visual and vibrotactile) stimulation (stimulation phase). Finally, the light turned red for a random duration of 5 to 7 seconds to indicate a resting phase. Each trial consisted of a warning (2 seconds), stimulation (2-4 seconds according to its intensity), and rest (5-7 seconds to avoid habituation) phases. Each participant performed 16 trials per-device configuration. Participants were instructed not to move or talk during the run.

D. EEG offline analysis

The offline analysis of the EEG signals was done with EEGlab v2022.1 [12] toolbox in Matlab R2021b. EEG files from one participant were not included due to an error in data acquisition resulting in data mislabeling. The raw EEG data were re-referenced using the Common Average Reference method, followed by a high-pass filter at 1 Hz. Then, a 50 Hz notch filter was applied, and data were downsampled to 512 Hz after applying an antialiasing low-pass filter at 256 Hz. Then, an independent component analysis (ICA) was performed to remove eye and muscle artifacts using the IClabel tool. This explains the high sampling rate chosen because it is recommended to have 20x(number of channels)^2 data points for the ICA analysis.

Then, epochs were extracted corresponding to 4.1 seconds before stimuli onset and 10 seconds afterward. The baseline was defined 4 seconds before the stimuli onset, and its duration was 2 seconds. The reasoning behind this choice is that participants had 2 seconds to prepare for the stimuli (see Section II-C), thus, some EEG activity may be present due to this period of anticipation. Each epoch was labeled according to the level of vibration intensity.

Once we had the epochs, we performed a time-frequency grand average analysis to observe the Event-Related Spectrum Perturbations (ERSPs). In this case, the baseline was defined at 500 ms before stimuli onset. The average was performed among participants (n=17) and the four vibration patterns. This analysis allowed us to identify the frequency bands with the most activity during the stimulation. Finally, we used these results to obtain topographies corresponding to the average duration of the stimulation to study the EEG activity over the cortex. We used the EEGlab statistics study tool to perform one-way repeated measures ANOVA with FDR correction and a statistical threshold (p-value) of 0.05 for the time-frequency ERSPs and 0.01 for the topographical analyses.

III. RESULTS

A. Time-Frequency analysis

Fig. 2 presents the results of time-frequency analyses for two electrodes placed over the central gyrus (namely C_3, C_4 in the 10-10 system), and two on the somatosensory cortex (CP_3, CP_4), corresponding respectively to the left and right hemispheres. As stated in [13], electrodes C_3 and C_4 report the activity in both, motor and sensory, primary cortex. We present results for four stimulation conditions, involving visual and vibrotactile stimuli: *None* condition, (2-second virtual hand grasp without ketchup or vibration), *Low* condition (2-second virtual hand grasp with little ketchup and low vibration), *Medium* condition (4-second virtual hand grasp with medium ketchup and medium vibration), and *High* condition (6-second virtual hand grasp with abundant ketchup and a high-intensity vibration). To avoid overlap with subsequent trials, the figures show a 3-second period after stimulus offset (resting phase) since the shortest stimulation duration is 2 seconds for the *None* and *Low* conditions. The time-frequency analyses provide averaged results for the four device configurations, which involve the activation of 2 or 3 vibration motors simultaneously or sequentially. Furthermore, separate time-frequency analyses were performed for each device configuration, but no significant differences were observed among them. Therefore, detailed results are not reported in this article.

1) Comparing locations: ERSPs for the *None* condition show an ERD primarily in the alpha band and the contralateral hemisphere, i.e., the right one (C_4, CP_4). The ERD continues even after stimuli offset at 2 seconds. Similarly, in the *Low* there is an ERD mainly in alpha, and a new ERD emerges in beta that lasts for two seconds. This alpha and beta activity is observed in all four electrodes, but the ERD weakens after the stimuli offset in CP_4 for alpha and in all electrodes for beta. During the *Medium* condition, the beta ERD is more pronounced in the contralateral hemisphere and CP_3, while it is less strong in C_3. Around 1 second after stimuli offset, an attenuation of the ERD is observed mainly on the contralateral hemisphere (C_4, CP_4), and an ERS emerges in the lower beta range (12-15 Hz) nearly 2 seconds after the offset. ERSPs for

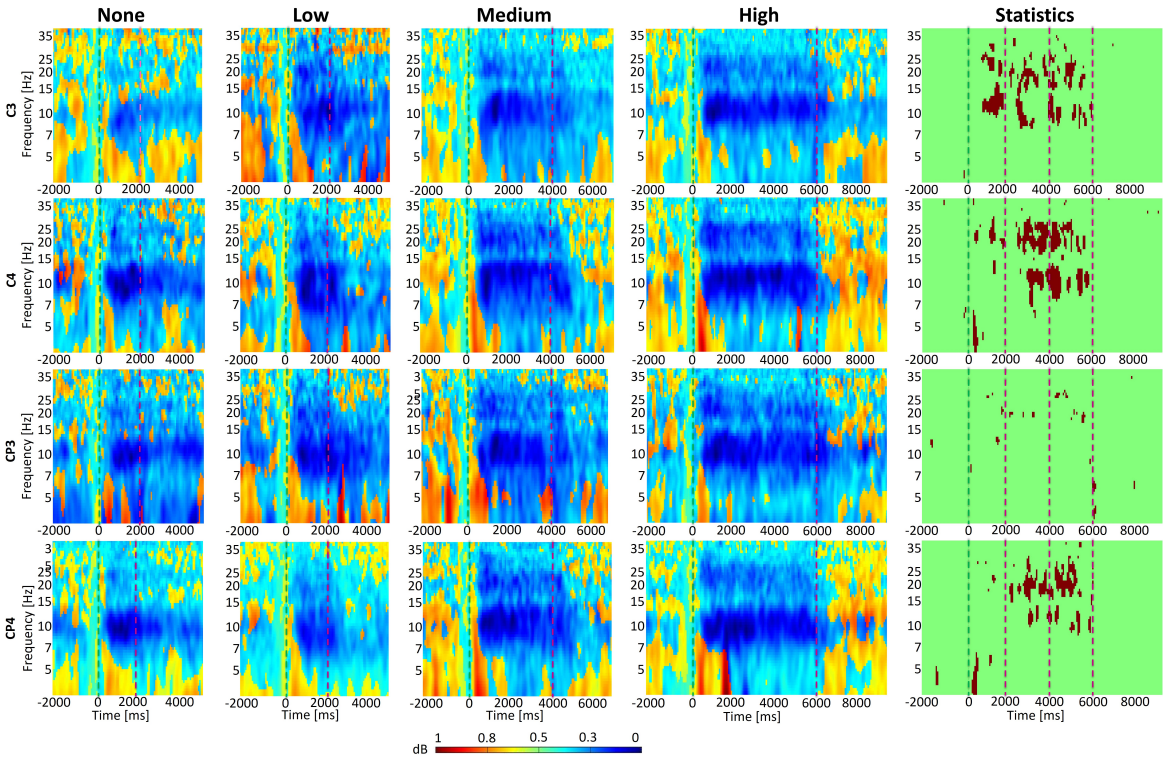

Fig. 2. ERSPs grand average time-frequency analysis (n=17) for electrodes C_3, C_4, CP_3, and CP_4 during the stimulation phase. Each column represents a different condition (*None*, *Low*, *Medium*, *High*), with the last column indicating statistically significant differences ($p < 0.05$) in ERSP values among conditions. The green dotted line indicates stimulation onset, while the red dotted line indicates stimulation offset. The graphs in the last column display multiple red dotted lines, representing different condition offsets: the first for *None* and *Low*, the second for *Medium*, and the last for *High*.

the *High* condition exhibit an ERD in the alpha and beta band, with alpha being more prominent. An ERS is visible on the beta band mainly in the contralateral hemisphere (C_4, CP_4), and in the postcentral ipsilateral area (CP_3) in alpha and beta. In summary, although alpha-related ERDs are observed in both hemispheres for all intensities, they are slightly stronger in the contralateral hemisphere and the postcentral ipsilateral area (CP_3).

2) Comparing intensities: Significant statistic test results (p=0.05) show several differences in activity among the intensity conditions.

- When the stimulation starts, a transient ERS is visible in the theta and delta bands in postcentral areas (CP_3, CP_4).
- The stimulation induces a decrease in power in the alpha and beta band in the somatomotor or somatosensory cortex (C_3, C_4), mainly on C_3 in the alpha band.
- When the stimulation stops for the *None* and *Low* conditions after 2 seconds, it continues for the *Medium* and *High* conditions, maintaining an ERD in the alpha and beta bands up to their end at 4 and 6 seconds, respectively.

B. Topographical analysis

During the time-frequency analysis, we observed relevant activity in the alpha and beta bands, but also an interesting increase of power at the beginning of the stimulation in the delta band, especially for the *Medium* and *High* conditions. Thus, we present the averaged topographies over the stimulation duration for alpha and beta in Fig. 3 and over an approximate duration of 1 second of delta's power increase in Fig. 4.

1) Activity in alpha and beta bands: Using time-frequency information from the ERSPs presented in the previous section, we computed topographies for 1) alpha (8-12 Hz) + low beta (12-15 Hz) and 2) high beta (15-25 Hz) for the first two seconds (Fig. 3). We averaged over the first 2 seconds of the stimulation because it was the duration of the shortest stimulation. Averaging over a longer period would involve the resting phase of the *None* and *Low* conditions. In the alpha+low beta band, a bilateral ERD is present in motor and somatosensory areas during the *Medium* and *High* conditions, while for the other two conditions, the ERD is weaker and contralateral. The ERDs in the *Medium*, and *High* conditions extend to the contralateral parietal lobe, corresponding to the somatosensory cortex. A contralateral decrease in power is visible for all conditions in the occipital lobe, maybe due to the left arm presented on the screen. Statistically significant differences among intensity conditions were observed in ipsilateral electrodes (C_3, FC_3, F_3). Pairwise Tukey comparisons performed in *jamovi* showed differences in C_3 between the *High-None* conditions ($p = 0.018$), and *Medium-None* ($p = 0.011$).

Regarding high beta, the ERD amplitude is lower than in al-

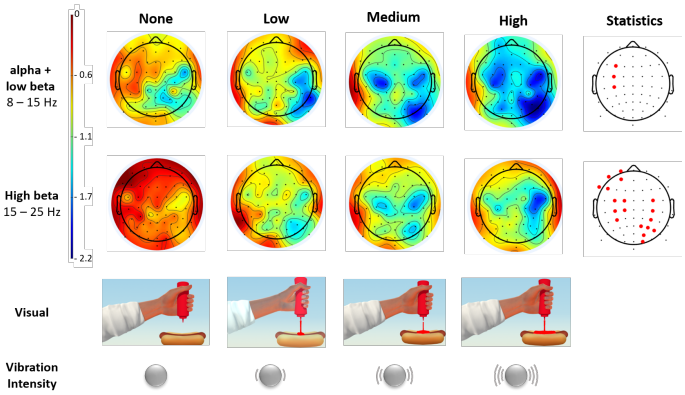

Fig. 3. Brain activity topographies averaged over two seconds (t=0-2000 ms). The first row represents the alpha+low beta band (8-15 Hz). The second row represents the high beta band (15-25 Hz). The third row displays visual animations for each condition, and the fourth row indicates vibration intensity. The first four columns correspond to the visual and vibration conditions, while the last column shows statistically significant differences ($p < 0.01$).

pha+low beta and is present only in the three conditions where the vibration was activated. This ERD is mainly contralateral and noticeable in the *High* condition, and it attenuates as the intensity of the stimulation decreases. Statistically significant differences ($p < 0.01$) are observed bilaterally in central and pre/postcentral areas corresponding to the somatomotor and somatosensory cortices, contralateral in posterior and some occipital electrodes. Pairwise Tukey comparisons exhibited differences in C_3 between: *High-Low* and *Medium-Low* both with $p < 0.05$, *High-None* ($p < 0.01$), and *Medium-None* ($p < 0.001$).

2) Activity in the delta band: Fig. 2 shows a strong transient ERS around the delta and theta bands in CP_3 and CP_4 at stimulation onset (t=0m s). To further study this phenomenon, we computed the averaged topographies over 0-1000 ms (Fig.4), corresponding to the first second of the stimulation for delta (1-4 Hz). We also computed the average topographies for the theta band (4-8 Hz) but the results are less significant. As we observed in the time-frequency analysis, the power increase is present only for the *High* and *Medium* conditions, mainly around C_z, CP_z, C_2, CP_2, and extending slightly to C_1, C_4, CP_1, CP_4, and FC_z.

IV. Discussion

A. The bimodal stimulation elicits bilateral ERDs in alpha and beta

We clearly observed bilateral ERDs elicited by visual and vibrotactile synchronized stimulation in the alpha and beta frequency bands (Fig. 2 and Fig. 3). The bilateral activity due to a vibrotactile stimulus was previously reported during focal vibration [14] and vibration with eyes open [6]. Thus, the activity we observe may be very well due to the visual stimulation. When comparing intensity conditions, a significant difference was observed only in 3 ipsilateral electrodes (Fig.3), probably due to the ipsilateral ERD present only in *Medium* and *High* conditions, while the contralateral ERD is constant

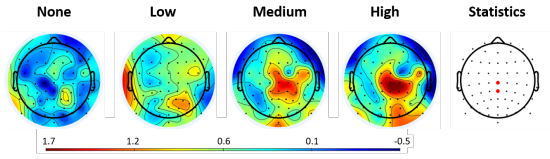

Fig. 4. Brain activity topographies averaged over the first second of the stimulation (0-1000 ms) in the 1-4 Hz delta band. The statistically significant differences ($p < 0.01$) are displayed in the right-most image.

in all conditions. Furthermore, this ipsilateral activity in the sensorimotor cortex increases with the contralateral occipital activity.

During the *None* condition (Fig. 2), an ERD is observed when the virtual hand movement starts, which has been previously reported for action observation [15]. Contrary to expectations, we did not observe an ERS once the stimulation was over for this condition. One possible explanation for this phenomenon is that the virtual hand reopens when the resting phase starts at 2000 ms. This may be interpreted as a second movement that elicits another ERD (the first one being the hand grasping the bottle), thus suppressing the ERS corresponding to the first movement. The vibration was not applied in this condition, therefore, the vibration stimulation cannot justify the absence of ERS. On the other hand, in the *Low* and *Medium* conditions, the ERD attenuates at stimuli offset, and an ERS becomes visible in the *High* condition. This may suggest that the appearance of this ERS is dependent on the vibration intensity.

The alpha-related ERDs present in all conditions are localized in the somatomotor and somatosensory cortices, so they may also correspond to the mu rhythm, which is present during motor and neurocognitive activities [16] and often mixed with central beta [17]. Lastly, the absence of an ERD in the high beta band for the *None* condition (Fig.3) suggests that vibration stimulus elicits EEG modulations in this frequency band rather than visual stimulus.

B. Presence of delta activity

A noteworthy finding is the significant transient ERS at the beginning of the stimulation in the delta band (Fig. 2). Traditionally, delta activity has been related to states of diminished consciousness [17]. However, it has also been suggested that delta oscillations are synchronized with visual cues timing [18].Yet, we only observed delta activity in the *Medium* and *High* conditions, and the visual cues were deliberately varied to prevent participant anticipation. Therefore, we cannot conclude that the delta activity solely resulted from the visual cues. Activity in the delta band has been previously reported during continuous-attention tasks [19] and during vibrotactile stimulation, suggesting it increased attention [6]. Given that we observed delta activity only in the *Medium* and *High* conditions, it is plausible that attention is dependent on the vibration intensity. Further studies on attention and vibrotactile stimulation are needed to substantiate this hypothesis.

C. Limitations and future work

We only studied bimodal stimulation, therefore it was impossible to differentiate brain activity resulting from the visual stimulus and the one from the vibrotactile stimulus except for the *None* condition. To gain further insights and isolate the effects of the vibration at different intensities, it would be valuable to perform a study comparing different stimulation modalities. Such research could enhance our understanding of how the brain processes vibrotactile information on the forearm and hand.

In our study, the virtual arm shown on the screen was the left one, which was to be the non-dominant. This may account for the contralateral occipital activity in both alpha and beta bands across all conditions, as well as the center-ipsilateral activity. Future experiments on the dominant right arm could validate our findings.

In upcoming work, we will incorporate our proposed bimodal stimulation into our functional KMI-based BCI (Fig. 1(a)) to assess its impact on BCI performance and user experience. In this context, the stimulation will serve as feedback because its intensity will depend on the brain activity during KMI. As demonstrated in this article, visual and vibrotactile stimulation elicits activity in the somatomotor and sensorimotor cortices. Therefore, feedback will be provided once the KMI task concludes to avoid overlapping of the brain activity. Furthermore, we will compare the bimodal feedback to visual-only and vibrotactile-only feedback, expecting variation in EEG oscillations during the feedback phase due to the distinct sensory modalities.

V. Conclusion

The different configurations of the vibrotactile device, based on the number of motors and activation sequence, did not yield statistically significant differences in brain activity. However, our study clearly observed brain activity in delta, alpha, and beta bands during our proposed novel visual and vibrotactile bimodal stimulation. Moreover, this activity exhibited variations depending on the stimulation intensity. Contrary to expectations, we observed bilateral brain activity, with the contralateral hemisphere demonstrating stronger activity. Notably, this activation encompassed not only central but also extended to pre/postcentral, posterior, and occipital areas. These findings provide valuable insights for optimizing the design of a BCI paradigm using our proposed bimodal stimulation as feedback for KMI of the upper limb and anticipate the brain responses associated with feedback modalities and intensities.

Acknowledgment

We thank the company Octarina for their contribution to the development of the graphic environments.

References

[1] S. Mansour, K. K. Ang, K. P. S. Nair, K. Soon Phua, and M. Arvaneh, "Efficacy of Brain-Computer Interface and the Impact of Its Design Characteristics on Poststroke Upper-limb Rehabilitation: A Systematic Review and Meta-analysis of Randomized Controlled Trials," *Clinical EEG and Neuroscience*, vol. 53, no. 1, pp. 79–90, 2022.

[2] C. M. Stinear, W. D. Byblow, M. Steyvers, O. Levin, and S. P. Swinnen, "Kinesthetic, but not visual, motor imagery modulates corticomotor excitability," *Experimental Brain Research*, vol. 168, no. 1-2, pp. 157–164, 1 2006. [Online]. Available: https://link.springer.com/article/10.1007/s00221-005-0078-y

[3] S. Le Franc, G. Herrera Altamira, M. Guillen, S. Butet, S. Fleck, A. Lécuyer, L. Bougrain, and I. Bonan, "Toward an Adapted Neurofeedback for Post-stroke Motor Rehabilitation: State of the Art and Perspectives," *Frontiers in Human Neuroscience*, vol. 16, 7 2022.

[4] W. Zhang, A. Song, H. Zeng, B. Xu, and M. Miao, "Closed-Loop Phase-Dependent Vibration Stimulation Improves Motor Imagery-Based Brain-Computer Interface Performance," *Frontiers in Neuroscience*, vol. 15, no. January, pp. 1–13, 2021.

[5] C. Schneider, R. Marquis, J. Jöhr, M. Lopes da Silva, P. Ryvlin, A. Serino, M. De Lucia, and K. Diserens, "Disentangling the percepts of illusory movement and sensory stimulation during tendon vibration in the EEG," *NeuroImage*, vol. 241, 11 2021.

[6] W. Li, Q. Xu, Y. Li, C. Li, F. Wu, and L. Ji, "EEG characteristics in "eyes-open" versus "eyes-closed" condition during vibrotactile stimulation," *Biomedical Signal Processing and Control*, vol. 68, p. 102759, 7 2021.

[7] G. Pfurtscheller and F. Lopes da Silva, "Event-related EEG/MEG synchronization and desynchronization: basic principles," *Clinical Neurophysiology*, vol. 110, no. 11, pp. 1842–1857, 11 1999.

[8] Y. G. Chung, J. Kim, S. W. Han, H.-S. Kim, M. H. Choi, S.-C. Chung, J.-Y. Park, and S.-P. Kim, "Frequency-dependent patterns of somatosensory cortical responses to vibrotactile stimulation in humans: A fMRI study," *Brain Research*, pp. 47–57, 2013.

[9] C. Jeunet, C. Vi, D. Spelmezan, B. N'Kaoua, F. Lotte, and S. Subramanian, "Continuous Tactile Feedback for Motor-Imagery Based Brain-Computer Interaction in a Multitasking Context," in *Lecture Notes in Computer Science()*, J. Abascal, S. Barbosa, M. Fetter, T. Gross, and M. Palanque, P.Winckler, Eds. Springer, Cham, 8 2015, vol. 9296, pp. 488–505.

[10] R. Leeb, K. Gwak, D. S. Kim, and J. D. R. Millan, "Freeing the visual channel by exploiting vibrotactile BCI feedback," *Proceedings of the Annual International Conference of the IEEE Engineering in Medicine and Biology Society, EMBS*, pp. 3093–3096, 2013.

[11] M. E. Johanson, M. A. James, and S. R. Skinner, "Forearm muscle activation during power grip and release," *The Journal of Hand Surgery*, vol. 23, no. 5, pp. 938–944, 9 1998.

[12] A. Delorme and S. Makeig, "EEGLAB: an open source toolbox for analysis of single-trial EEG dynamics including independent component analysis," *Journal of Neuroscience Methods*, vol. 134, pp. 9–21, 2004. [Online]. Available: http://www.sccn.ucsd.edu/eeglab/

[13] N. P. Holmes and L. Tamè, "Locating primary somatosensory cortex in human brain stimulation studies: systematic review and meta-analytic evidence," *Journal of Neurophysiology*, vol. 121, no. 1, pp. 152–162, 1 2019.

[14] W. Li, C. Li, Q. Xu, L. Ji, and S. Cunningham, "Effects of Focal Vibration over Upper Limb Muscles on the Activation of Sensorimotor Cortex Network: An EEG Study," *Journal of Healthcare Engineering*, vol. 2019, 2019.

[15] P. Avanzini, M. Fabbri-Destro, R. Dalla Volta, E. Daprati, G. Rizzolatti, and G. Cantalupo, "The Dynamics of Sensorimotor Cortical Oscillations during the Observation of Hand Movements: An EEG Study," *PLoS ONE*, vol. 7, no. 5, p. e37534, 5 2012.

[16] C. Neuper, R. Scherer, S. Wriessnegger, and G. Pfurtscheller, "Motor imagery and action observation: Modulation of sensorimotor brain rhythms during mental control of a brain–computer interface," *Clinical Neurophysiology*, vol. 120, no. 2, pp. 239–247, 2 2009.

[17] E. Niedermeyer and F. Lopes da Silva, Eds., *Electroencephalography: basic principles, clinical applications, and related fields*, 5th ed. Philadelphia: Lippincott Williams & Wilkins, 2005.

[18] M. Saleh, J. Reimer, R. Penn, C. L. Ojakangas, and N. G. Hatsopoulos, "Fast and Slow Oscillations in Human Primary Motor Cortex Predict Oncoming Behaviorally Relevant Cues," *Neuron*, vol. 65, no. 4, pp. 461–471, 2 2010.

[19] E. Kirmizi-Alsan, Z. Bayraktaroglu, H. Gurvit, Y. H. Keskin, M. Emre, and T. Demiralp, "Comparative analysis of event-related potentials during Go/NoGo and CPT: Decomposition of electrophysiological markers of response inhibition and sustained attention," *Brain Research*, vol. 1104, no. 1, pp. 114–128, 8 2006.